

Supplementary Information for:

SDS-Assisted Protein Transport Through Solid-State Nanopores

Laura Restrepo-Pérez^{1†}, Shalini John^{2†}, Aleksei Aksimentiev^{2*}, Chirlmin Joo^{1*}, Cees Dekker^{1*}

¹ Department of Bionanoscience, Kavli Institute of Nanoscience, Delft University of Technology, van der Maasweg 9, 2629 HZ Delft, The Netherlands

² Department of Physics, University of Illinois at Urbana; Champaign, Urbana, Illinois 61801, United States

Table of Contents

Table S1: Summary of MD simulations of nanopore systems.	2
Figure S1. MD simulation of folded titin translocation	3
Figure S2. Simulated ionic current blockades produced by translocation of molecular species through a 6 nm diameter nanopore.....	5
Figure S3. Simulated ionic current blockades in a 10 nm-diameter nanopore.....	6
Note S1. Estimation of the critical micelle concentration of SDS using dynamic light scattering (DLS)	7
Figure S4. DLS measurements of micelle hydrodynamic radius at different SDS concentrations.....	7
Note S2. Tryptophan fluorescence bulk assay.....	8
Figure S5. Tryptophan fluorescence bulk measurements of β -amylase at different SDS concentrations.....	8
Note S3. Characterization of SDS micelles in nanopores.....	9
Figure S6. Translocation of SDS micelles.....	9
Figure S7. Translocation of native and SDS-unfolded titin.....	10
Figure S8. Simulated ionic current blockades produced by a stretched peptide chain.	11
Captions to animations of MD trajectories.....	12

Table S1: Summary of MD simulations of nanopore systems.

Nanopore and membrane dimensions	Biomolecules	Number of atoms	Transmembrane bias (mV)	Simulation time (ns)		
System 1: Membrane cross section: 15 nm x 15 nm Membrane thickness: 6 nm Inner pore diameter: 6 nm Outer pore diameter: 7.5 nm	SDS micelle (70 SDS molecules)	322,601	125	130		
			250	80		
			500	20		
	Folded titin, conf. 1	330,898	500	60		
			-500	60		
	Folded titin, conf. 2	338,624	500	60		
			-500	60		
	SDS/titin, conf. 1 (76 SDS molecules)	340,937	125	160		
			250	130		
	SDS/titin, conf. 2 (76 SDS molecules)	344,343	125	250		
			250	125		
	SDS/titin dimer, conf. 1 (104 SDS molecules)	395,308	125	160		
			250	120		
SDS/titin dimer, conf. 2 (104 SDS molecules)	416,979	125	140			
		250	120			
SDS/ β -amylase, conf. 1 (249 SDS molecules)	558,595	500	110			
		500	120			
		500	160			
System 2: Membrane cross section: 15 nm x 15 nm Membrane thickness: 10 nm Inner pore diameter: 10 nm Outer pore diameter: 13 nm	SDS micelle (70 SDS molecules)	290,558	500	50		
			Folded titin	291,193	500	50
					500	50
Folded β -amylase	290,155	500	50			
		500	50			
SDS/ β -amylase, conf. 2 (249 SDS molecules)	351,622	500	50			
		500	50			
SDS/ β -amylase, orient. 1 (249 SDS molecules)	411,720	500	50			
		500	50			
SDS/ β -amylase, orient. 2 (249 SDS molecules)	389,398	500	50			
		500	50			
SDS/ β -amylase, orient. 3 (249 SDS molecules)	358,543	500	50			
		500	50			

Figure S1. MD simulation of folded titin translocation

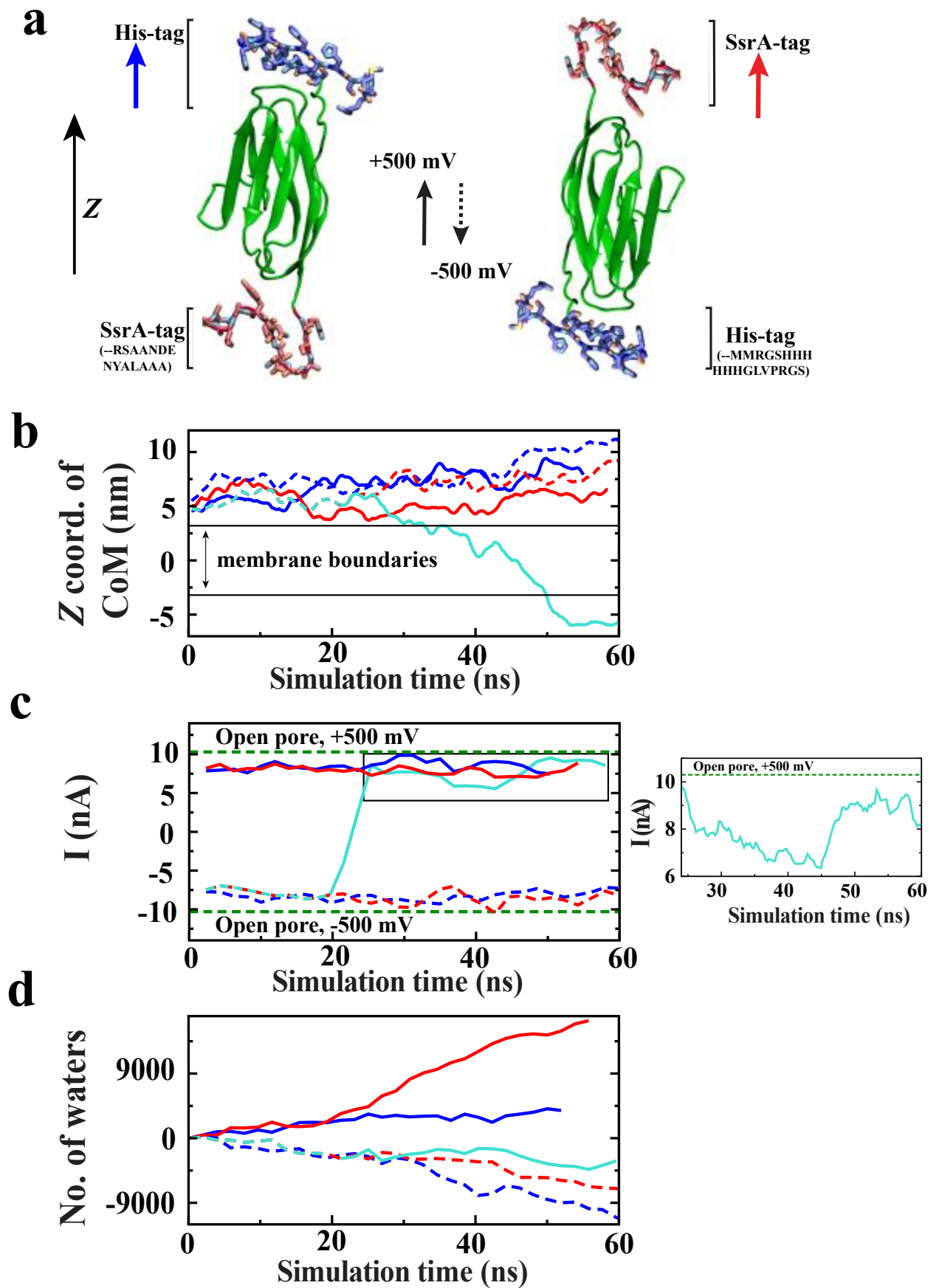


Figure S1. MD simulation of folded titin translocation. (a) Molecular structure of the folded titin monomer. To reproduce the constructs used in experiment, SsrA and His tags were added to the C and N terminals of the protein, respectively. The blue and red arrows define the initial orientation of the protein with respect to the z-axis of our setup (shown in black), which is also the direction of a positive transmembrane bias. (b-d) MD simulation of folded titin translocation through a 6 nm diameter nanopore (System 1). (b) The z coordinate of the titin's center of mass as a function of simulation time. The horizontal black lines indicate the location of the membrane. The color and the style (solid/dashed) of the lines indicate the initial orientation of the protein and the direction of the transmembrane bias, respectively, defined in panels a. In one simulation (gray), the bias was switched during the MD simulation. Each translocation traces shows a 1-ns running average of 4.8 ps sampled data. (c) The nanopore ionic current recorded in the simulations of folded titin translocation. Each ionic current trace shows a 5 ns running average of 4.8 ps sampled instantaneous current. The inset on the right shows a zoomed-in view of the ionic current trace for the fragment of the MD trajectory where protein translocation was observed (black rectangle in the main plot). In the inset, the ionic current trace shows 1 ns running average of 4.8 ps sampled instantaneous currents. (d) The total number of water molecules that passed through the nanopore from the beginning of the applied bias simulation. In this panel, positive values indicate net water flux in the direction of the z axis. The direction of the water flux is correlated with the sign of the transmembrane bias, indicating an electro-osmotic flow produced by a negatively charged nanopore surface.

Figure S2. Simulated ionic current blockades produced by translocation of molecular species through a 6 nm diameter nanopore

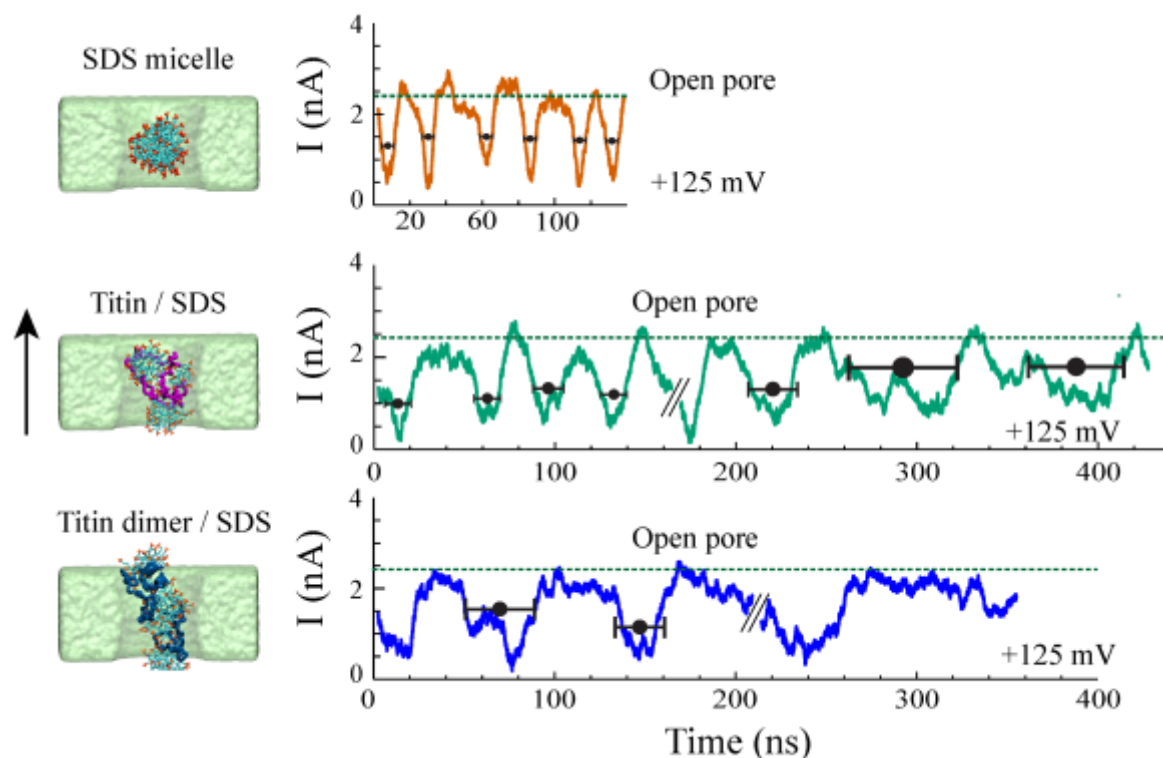


Figure S2. Simulated ionic current blockades produced by translocation of molecular species through a 6 nm diameter nanopore. Left column illustrates typical microscopic conformations observed during nanopore translocation simulations; the black arrow indicated the direction of the positive transmembrane bias. The conformation of a protein is depicted as a trace of the protein backbone; SDS molecules are shown as molecular bonds; water and ions are not shown for clarity. Right columns shows the ionic current traces recorded from the translocation simulations and the open pore current levels. Because of the periodic boundary conditions employed in our MD simulations, individual ionic current traces feature multiple translocation events. Ionic current traces from independent simulations are delineated by the “//” mark. Black circles and horizontal black bars indicate the average blockade current of individual blockade events and the duration of each event, respectively. The blockade events were defined by the reduction of the nanopore current below 75% of the open pore value.

Figure S3. Simulated ionic current blockades in a 10 nm-diameter nanopore

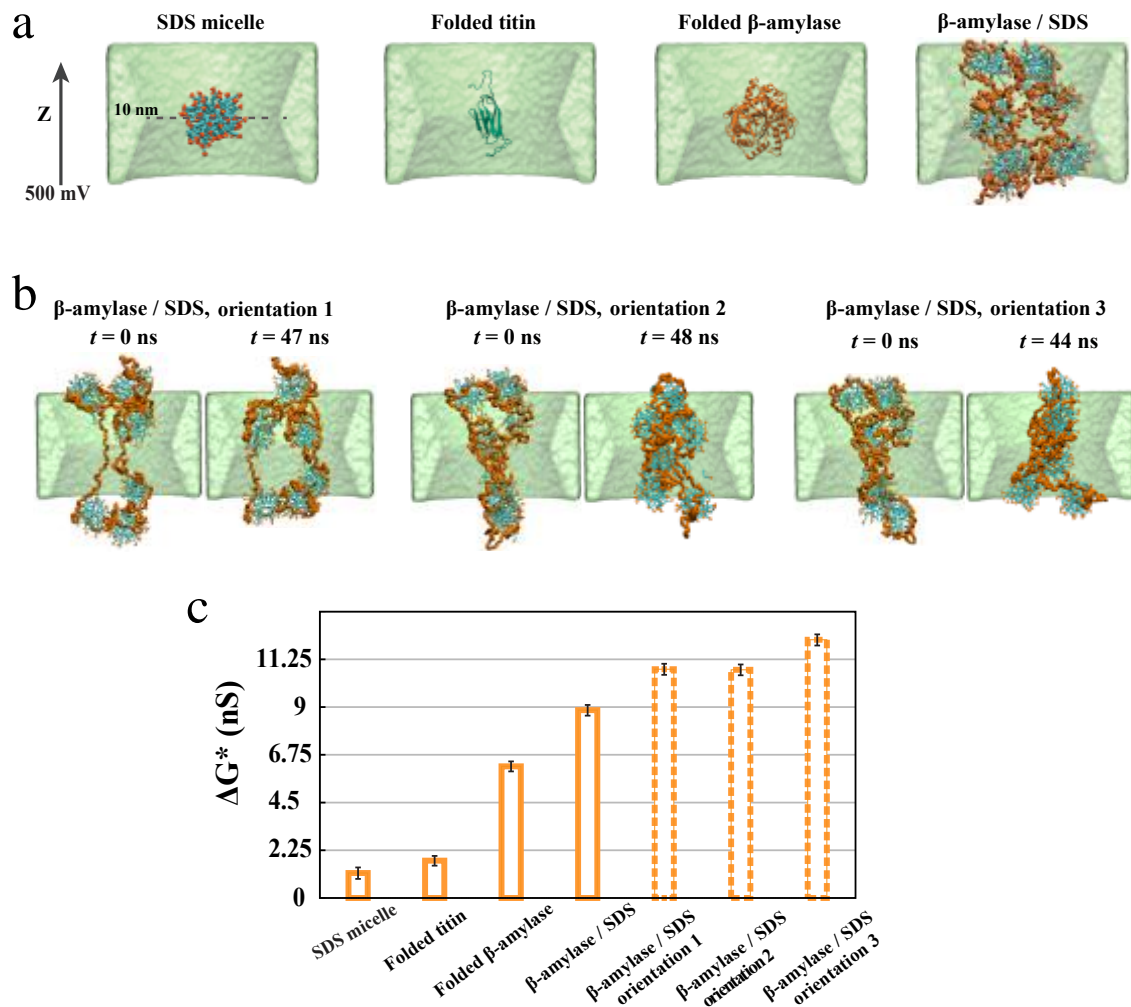


Figure S3. Simulated ionic current blockades in a 10 nm-diameter nanopore. (a) Molecular configurations used for the simulation of the ionic current blockades. The center of mass of each molecule or molecular assembly was restrained to the center of the nanopore. Water and ions are not shown for clarity. (b) Additional simulations of β -amylase/SDS blockade currents. The initial conformations of the β -amylase/SDS assemblies were taken from the translocation simulations performed using the 6 nm-diameter nanopore (System 1). In each 48-ns simulation, the center of mass of the β -amylase/SDS assembly was restrained to the center of the nanopore. (c) The average conductance blockade amplitudes. To enable direct comparison with experiment, the conductance blockades computed from MD simulations were multiplied by the ratio of the experimental and simulation bulk conductivities of 0.4 KCl (3.6/4.8). The average blockade conductance amplitudes were each computed from a 48 ns MD trajectory.

Note S1. Estimation of the critical micelle concentration of SDS using dynamic light scattering (DLS)

It is well known that SDS critical micelle concentration is dependent on the ionic strength of the solution. The formation of micelles depends on the interplay between the attractive forces driven by hydrophobic interactions of the hydrocarbon tails and the repulsive electrostatic interaction between the charged heads. At high ionic concentrations, charges are screened and the critical micelle concentration is reduced. To determine the CMC of SDS in the buffer used for our experiments, we used DLS to determine at which concentrations we notice the presence and absence of SDS micelles.

DLS measurements were performed using a Malvern Instruments Zetasizer Nano ZS. Samples containing different SDS concentration were prepared in a buffer containing 0.4M NaCl, 10mM TRIS and 1mM ETDA pH 7.5. The hydrodynamic radius of each sample was measured and is presented in Figure S4. For SDS concentrations higher than 0.05% micelles were observed with the expected hydrodynamic radius. No micelles were observed below 0.01% SDS. These results indicate a CMC for SDS in the range of 0.01% - 0.05%.

Figure S4. DLS measurements of micelle hydrodynamic radius at different SDS concentrations.

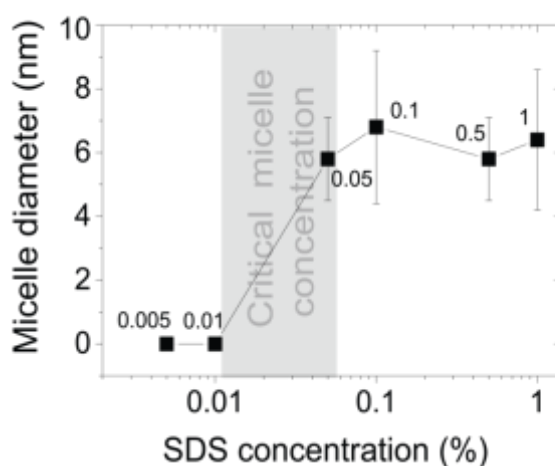


Figure S4. DLS measurements of micelle hydrodynamic radius at different SDS concentrations. The presence of micelles above 0.05% SDS and their absence below 0.01% SDS marks the region where the CMC is located.

Note S2. Tryptophan fluorescence bulk assay

Tryptophan fluorescence is routinely used to study protein conformational changes. Tryptophan fluorescence emission is highly dependent on the nature of its local environment, which can be used to infer the conformation of a protein. In a native or folded protein, most tryptophan residues are either partially or fully buried in the core of the protein due to their hydrophobic nature. Once the protein is unfolded with denaturing agents such as SDS or urea, tryptophan residues become partially or fully exposed and their fluorescent emission shifts. Here we used this principle to study the effect of SDS at different concentrations on one of our protein substrates.

All our measurements were done in a solution containing 0.4 M NaCl, 10mM Tris pH 7.5, 1mM EDTA, 1mM of DTT and different concentrations of SDS as shown in the following figure. Fluorescent measurements were done in a Cary eclipse fluorescence spectrophotometer with an excitation wavelength of 295nm and emission collected from 300nm – 450nm. The buffer background was measured and subtracted from each protein measurement.

Figure S5. Tryptophan fluorescence bulk measurements of β -amylase at different SDS concentrations

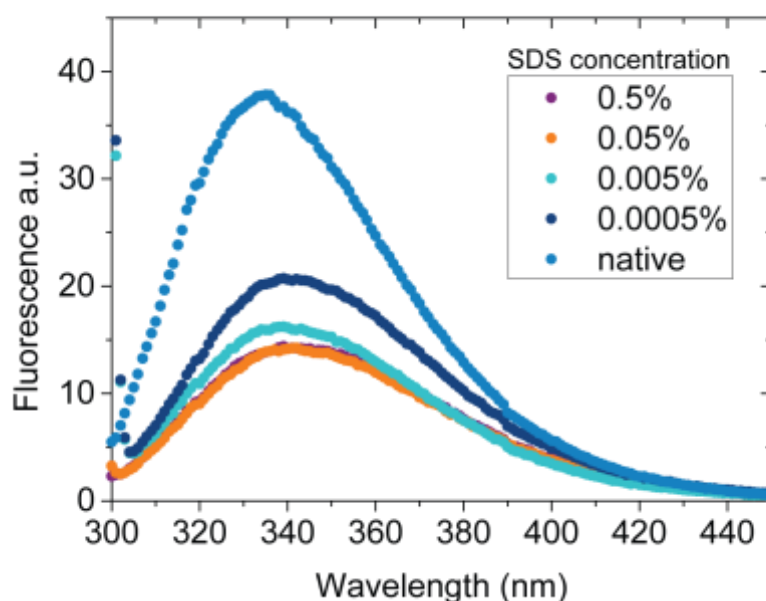


Figure S5. Tryptophan fluorescence bulk measurements of β -amylase at different SDS concentrations. A clear conformational change is observed in the protein even at SDS concentrations below CMC.

Note S3. Characterization of SDS micelles in nanopores

We performed control experiments to study the translocation of SDS micelles through solid-state nanopores in the absence of proteins. The experimental set up and a typical current trace are shown in Figure S6a and Figure S6b respectively. The scatter plot in Figure S6c shows the amplitude vs. dwell time for both SDS micelles alone and SDS-treated proteins. The conductance blockade histogram is presented in Figure S6d.

Figure S6. Translocation of SDS micelles

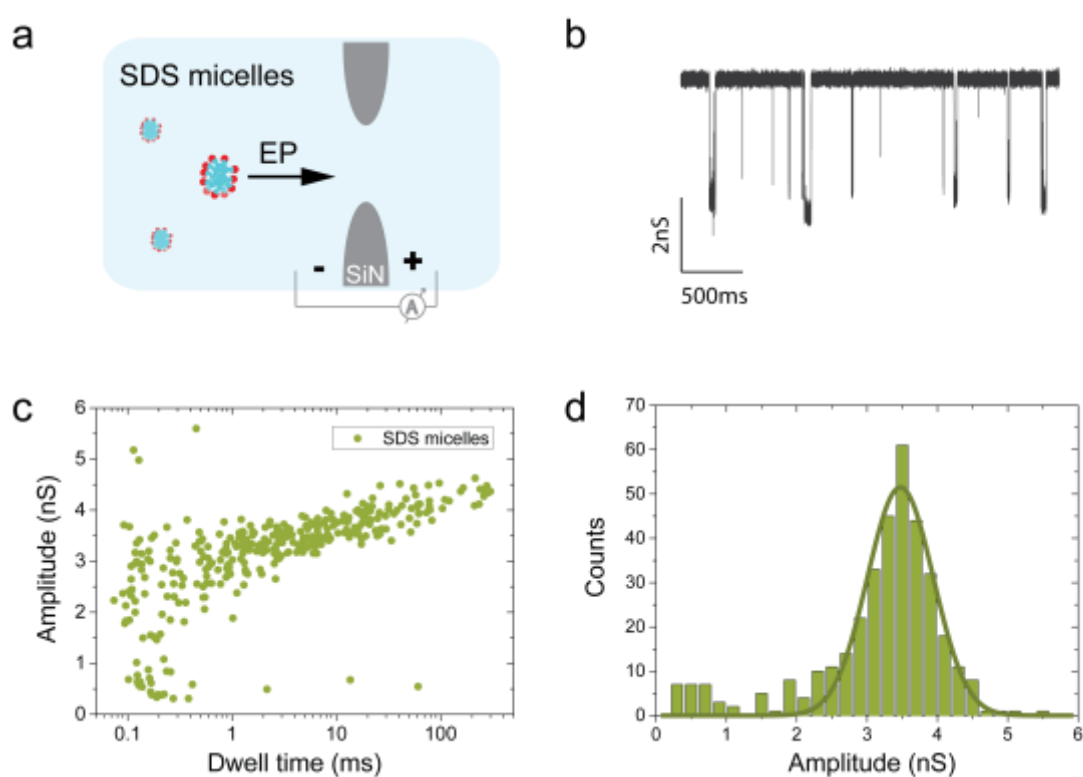


Figure S6. Translocation of SDS micelles (a) Schematic representation of the nanopore control experiment. (b) Example of a current trace measured showing the translocation of SDS micelles. (c) Dwell time vs. conductance blockade scatter plot for SDS-micelles and SDS-treated protein. (d) Conductance blockade histogram of the translocation of micelles.

Figure S7. Translocation of native and SDS-unfolded titin

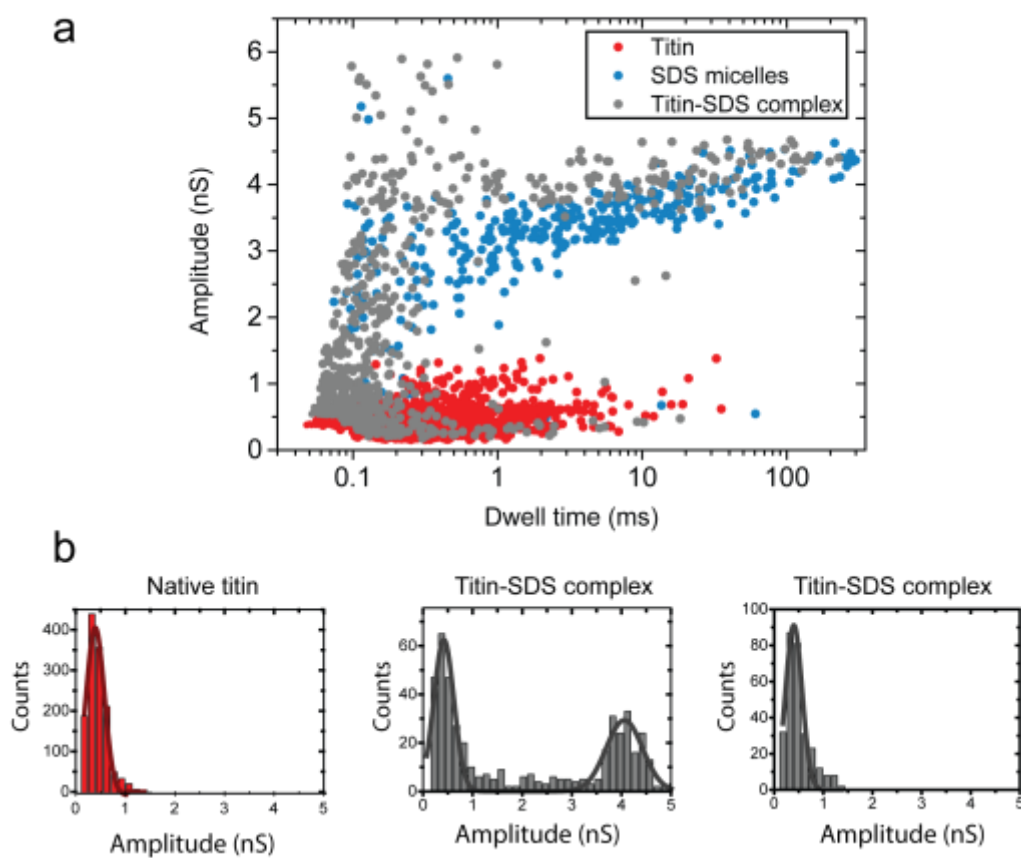


Figure S7. Translocation of native and SDS-unfolded titin. (a) Scatter plots of dwell time vs. conductance blockade for titin, SDS-titin and SDS micelles. (b) Histograms of the amplitude of the blockade for native titin (left), SDS-titin at an SDS concentration above CMC (middle) and SDS-titin below CMC (right).

Figure S8. Simulated ionic current blockades produced by a stretched peptide chain.

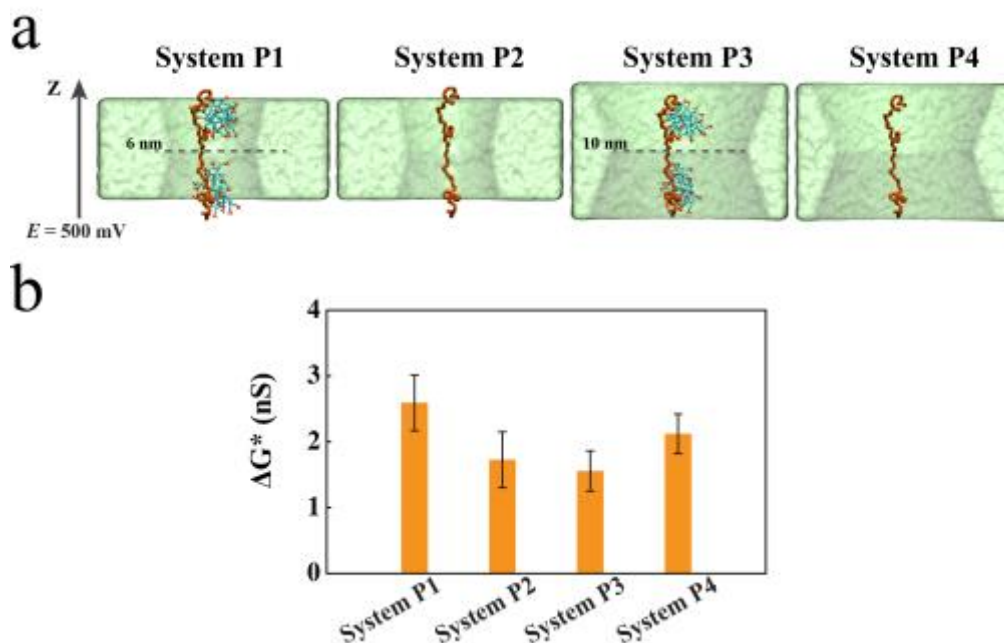


Figure S8. Simulated ionic current blockades produced by a stretched peptide chain. (a) Molecular configurations featuring a 60 amino acid fragment of β -amylase (residues 10 to 70) with (Systems P1 and P3) and without (Systems P2 and P4) attached SDS molecules threaded through either the 6 nm diameter nanopore (Systems P1 and P2) or the 10 nm diameter nanopore (Systems P3 and P4). The initial configuration of the peptide was taken from the simulation of the β -amylase/SDS assembly, orientation 3 at $t = 0$ ns (see Figure S3). The center of mass of the peptide chain/SDS assembly (Systems P1 and P3) or only of the peptide chain (Systems P2 and P4) was aligned with the geometrical center of each nanopore. During MD simulations of the ionic current, the backbone atoms of the peptide chain were harmonically restrained to their initial coordinates; SDS molecules were not restrained. At the end of the 60 ns simulations of Systems P1 and P3 under a 500 mV transmembrane bias, 20 and 1 SDS molecules detached from the peptide chain, respectively. (b) The average conductance blockade amplitudes. To enable direct comparison with experiment, the conductance blockades computed from MD simulations were multiplied by the ratio of the experimental and simulation bulk conductivities of 0.4 KCl (3.6/4.8). The average blockade conductance amplitudes for each system were computed from a 60 ns MD trajectory.

Captions to animations of MD trajectories.

Movie 1. Self-assembly of a titin-SDS complex. The movie illustrates a 300 ns explicit solvent all-atom MD simulation. The protein backbone is shown in blue, SDS molecules in cyan and red, water and 0.4 M NaCl are now shown. A smoothing filter was applied to visually reduce thermal motion of the molecules. The initial configuration was prepared by combining an unfolded conformation of a protein with 120 randomly distributed SDS molecules. The systems were simulated at 373 K for the first 200 ns. Following that, the systems were cooled down to 300 K in eight simulation runs, decreasing the system's temperature by 10 K between each run. Following that, the SDS-protein systems were simulated for another 50 ns at 300 K.

Movie 2. MD simulation of folded titin translocation. The movie illustrates a 60 ns explicit solvent all-atom MD simulation carried out under a 500 mV bias directed from the bottom to the top of the simulation system. The nanopore is shown as a cutaway green molecular surface, the protein (red) is shown in a cartoon representation, water and 0.4 M NaCl are now shown. During the simulation, the center of mass of the protein was restrained to remain at the symmetry axis of the nanopore.

Movie 3. MD simulation of SDS-titin complex translocation. The movie illustrates a 100 ns explicit solvent all-atom MD simulation carried out under a 250 mV bias directed from the bottom to the top of the simulation system. The nanopore is shown as a cutaway green molecular surface; the protein conformation is depicted as a trace of the protein backbone (magenta). The SDS molecules are shown using the molecular bonds representation: Carbon, sulfur and oxygen atoms are shown in cyan, yellow and red, respectively, hydrogen atoms are not shown. Water and 0.4 M NaCl are now shown as well. During the simulation, the center of mass of the SDS-protein complex was restrained to remain at the symmetry axis of the nanopore. A smoothing filter was applied to visually reduce thermal motion of the molecules. Because of the periodic boundary conditions employed in our MD simulations, the same SDS-protein complex is seen to permeation through the nanopore multiple times. Flickering of the molecules is produced by crossings between different periodic images of the simulation unit cell.

Movie 4. MD simulation of SDS-titin dimer complex translocation. The movie illustrates a 50 ns explicit solvent all-atom MD simulation carried out under a 250 mV bias directed from the bottom to the top of the simulation system. The nanopore is shown as a cutaway green molecular surface; the protein conformation is depicted as a trace of the protein backbone (light blue). The SDS molecules are shown using the molecular bonds representation: Carbon, sulfur and oxygen atoms are shown in cyan, yellow and red, respectively, hydrogen atoms are not shown. Water and 0.4 M NaCl are now shown as well. During the simulation, the center of mass of the SDS-protein complex was restrained to remain at the symmetry axis of the nanopore. A smoothing filter was applied to visually reduce thermal motion of the molecules. Because of the periodic boundary conditions employed in our MD simulations, the same SDS-protein complex is seen to permeation through the nanopore multiple times. Flickering of the molecules is produced by crossings between different periodic images of the simulation unit cell.

Movie 5. MD simulation of SDS-beta amylase complex translocation. The movie illustrates a 150 ns explicit solvent all-atom MD simulation carried out under a 500 mV

bias directed from the bottom to the top of the simulation system. The nanopore is shown as a cutaway green molecular surface; the protein conformation is depicted as a trace of the protein backbone (magenta). The SDS molecules are shown using the molecular bonds representation: Carbon, sulfur and oxygen atoms are shown in cyan, yellow and red, respectively, hydrogen atoms are not shown. Water and 0.4 M NaCl are now shown as well. During the simulation, the center of mass of the SDS-protein complex was restrained to remain at the symmetry axis of the nanopore. A smoothing filter was applied to visually reduce thermal motion of the molecules. Because of the periodic boundary conditions employed in our MD simulations, the same SDS-protein complex is seen to permeation through the nanopore multiple times. Flickering of the molecules is produced by crossings between different periodic images of the simulation unit cell.

Movie 6. MD simulation of SDS micelle translocation. The movie illustrates a 85 ns explicit solvent all-atom MD simulation carried out under a 250 mV bias directed from the bottom to the top of the simulation system. The nanopore is shown as a cutaway green molecular surface. The SDS molecules are shown using the molecular bonds representation: Carbon, sulfur and oxygen atoms are shown in cyan, yellow and red, respectively, hydrogen atoms are not shown. Water and 0.4 M NaCl are now shown as well. During the simulation, the center of mass of the SDS micelle was restrained to remain at the symmetry axis of the nanopore. A smoothing filter was applied to visually reduce thermal motion of the molecules. Because of the periodic boundary conditions employed in our MD simulations, the micelle is seen to permeation through the nanopore multiple times. Flickering of the molecules is produced by crossings between different periodic images of the simulation unit cell.